CHAPTER IV
RESULTS AND DISCUSSION

4.1 Micellar Formation

Micellar formation was carried out to determine CMC of CTAT surfactant. Figure 4.1 shows a plot of surface tension against log concentration of CTAT. As expected, the graph shows that surface tension decreases with increasing CTAT concentration. At concentration above the CMC, the surface tension remains fairly constant. The CMC of CTAT obtained was 0.011 %wt at 30 °C.

A similar result was also obtained by conductivity measurement, with a CMC value of 0.01%wt. The plot of conductivity againsts surfactant concentrations is linear, with a break at the CMC, above which the decreased slope of the plot becomes linear again (see Figure 4.2). The break in the plot is due to the binding of some of the counterions to the micelle. For CTAT, the degree of binding of tosilate group to the micelle is ≈ 0.75 at 30 °C.

Soltero *et al.* (1995) studied the phase behavior of CTAT and water. They found that the plots of conductivity as a function of surfactant concentration show two breaks. The first break signal is CMC the formation of spherical micelles about 0.011 %wt. The second break corresponds to a transition from spherical to cylindrical micelles about 0.04 %wt. The temperature-composition phase diagram of binary mixtures of CTAT and water showed the end of surfactant concentration which formed cylindrical micelles at 25 %wt. CMC of CTAT obtained from this work was consistent with CMC obtained by Becerra *et al.* (2003) and Soltero *et al.* (1995). Therefore the amount of CTAT selected for this work was 5 %wt, 10 %wt, and 25 %wt which were higher than 0.04 %wt to be certain that wormlike micelles were obtained in the system.

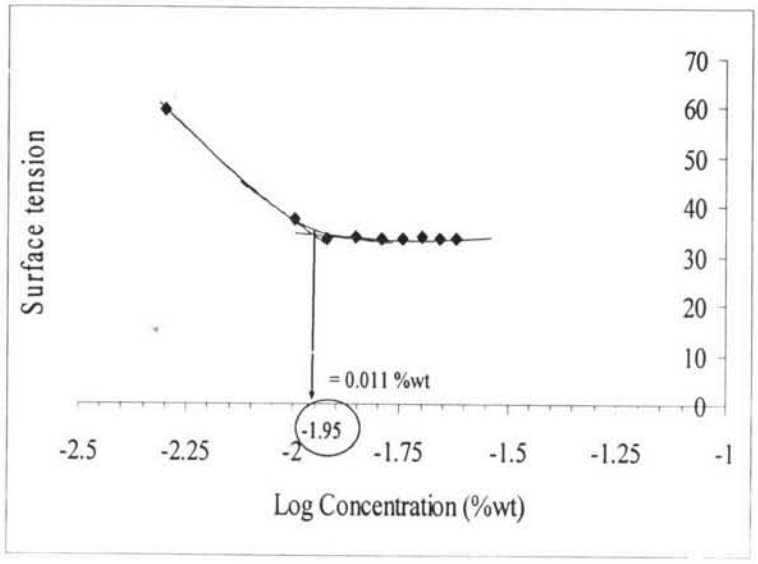

Figure 4.1 Surface tension of CTAT solution as a function of surfactant concentration at 30±1 °C.

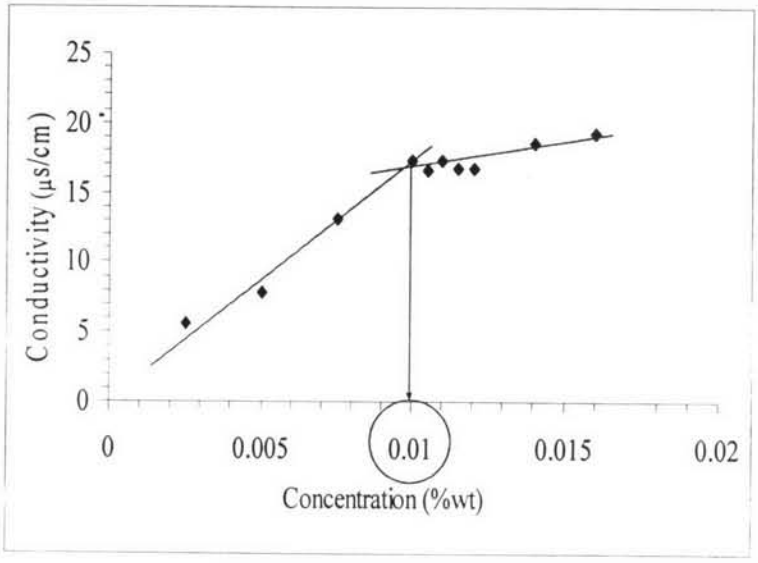

Figure 4.2 Conductivity of CTAT solution as a function of surfactant concentration 30±1 °C.

4.2 Micellar Polymerization

Polymerization conditions selected in this study were established after CMC of the CTAT was determined. The polymerization conditions were selected to study the effect of different variables had on the morphology of the obtained polystyrene stabilized wormlike micelles and the obtained polymers. Effect of the CTAT concentrations, initiator loading and styrene loading on molecular weight of the obtained polystyrene were further investigated by GPC and TEM was used to study the impact of these variables on morphology of the polystyrene stabilized wormlike micelle.

At low surfactant to styrene loading (6:1), very little polymer was produced at any of the initiator ratios or polymerization temperatures studied. The amount obtained polymers were relatively small and were not enough to carry out any further characterizations. The obtained polymers were found on the solution surface and assembled to give an ultra-thin film as observed in Figure 4.3. The visual characteristics of the obtained polystyrene are presented in Table 4.1.

Table 4.1 Polymerization conditions and the characteristic of polystyrene obtained

CTAT (wt.%)	Styrene: AIBN (mole: mole)	Styrene loading (mole CTAT: mole Styrene)	Temperature (°C)	Visual Appearance
5	15:1	Low loading (6:1)	70	ultra-thin film
	30:1		70	ultra-thin film
	50:1		70	ultra-thin film
	15:1	Medium loading (3:1)	70	ultra-thin film
	30:1		70	ultra-thin film
	50:1		70	ultra-thin film
	15:1	High loading (1.6:1)	70	suspension and sediment
	30:1		70	suspension and sediment
	50:1		70	suspension and sediment
10	15:1	Low loading (6:1)	70	ultra-thin film
	30:1		70	ultra-thin film
	50:1		70	ultra-thin film
	15:1	Medium loading (3:1)	70	suspension and sediment
	30:1		70	ultra-thin film
	50:1		70	ultra-thin film
	15:1	High loading (1.6:1)	70	suspension and sediment
	30:1		70	suspension and sediment
	50:1		70	suspension and sediment

Table 4.1 Polymerization conditions and the characteristic of polystyrene obtained (cont.)

CTAT (wt.%)	Styrene: AIBN (mole: mole)	Styrene loading (mole CTAT: mole Styrene)	Temperature (°C)	Visual Appearance
20	15:1	Low loading (6:1)	70	suspension and sediment
	30:1		70	suspension and sediment
	50:1		70	suspension and sediment
	15:1	Medium loading (3:1)	70	suspension and sediment
	30:1		70	suspension and sediment
	50:1		70	suspension and sediment
	15:1	High loading (1.6:1)	70	suspension and sediment
	30:1		70	suspension and sediment
	50:1		70	suspension and sediment
	50:1		60	ultra-thin film
	50:1		50	ultra-thin film

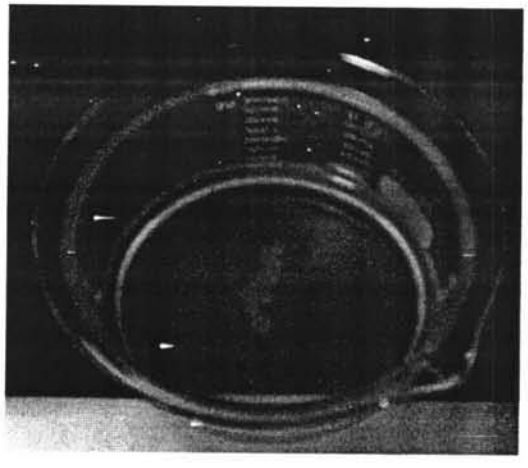

Figure 4.3 Photograph of polystyrene on solution surface.

4.3 Characterization of Obtained Polystyrene

4.3.1 Fourier Transform Infrared Spectroscopy Results

In order to confirm the formation of polystyrene, the obtained polymer sample was investigated by FTIR. The FTIR spectrum of CTAT and a polystyrene sample are shown in the Figure 4.4 and 4.5, respectively.

Figure 4.4 shows the spectrum of a sample which was polymerized in 20 %wt of CTAT and high styrene loading (1.6:1). The result shows that all peaks observed in the sample were consistent with the spectrum of the polystyrene standard. It clearly show all characteristic of polystyrene i.e. the benzene ring with the aromatic C-H stretching at 3100-3000 cm^{-1}, aromatic C=C stretching at1600 cm^{-1} , 1495 cm^{-1}, 1454 cm^{-1}, and out of plane aromatic C-H bending at 700 cm^{-1}.

It was interesting to note that characteristic symmetric S-O stretching peak of CTAT at 1190 cm^{-1} was also observed in all spectra of polystyrene samples. This was probably due to some CTAT trapped in the polystyrene sample during the precipitation process (see Figure 4.5).

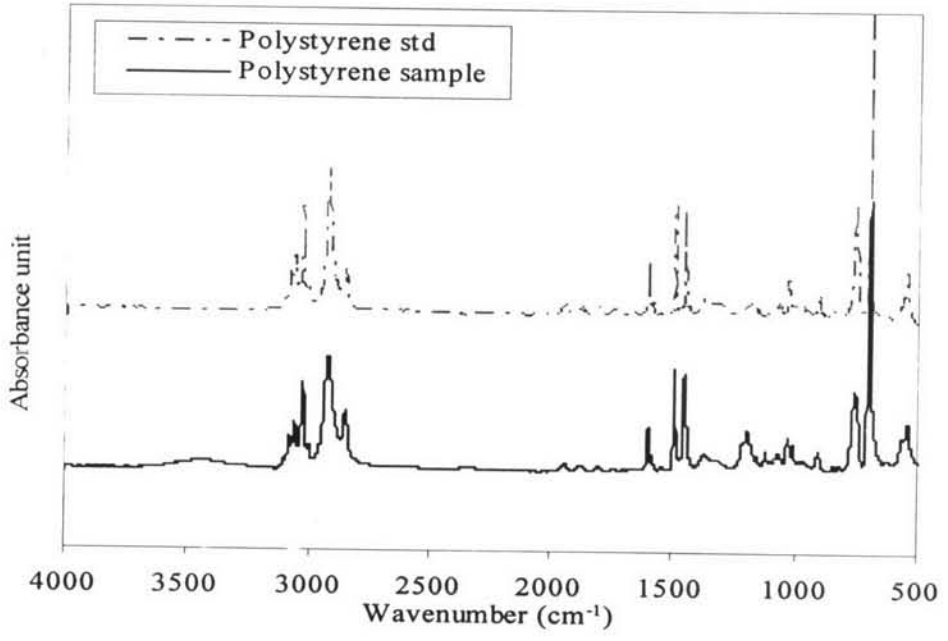

Figure 4.4 FTIR spectrum of polystyrene standard and polystyrene in 20 %wt CTAT, 15:1 of styrene to AIBN ratio, and 1.6:1 of CTAT to styrene.

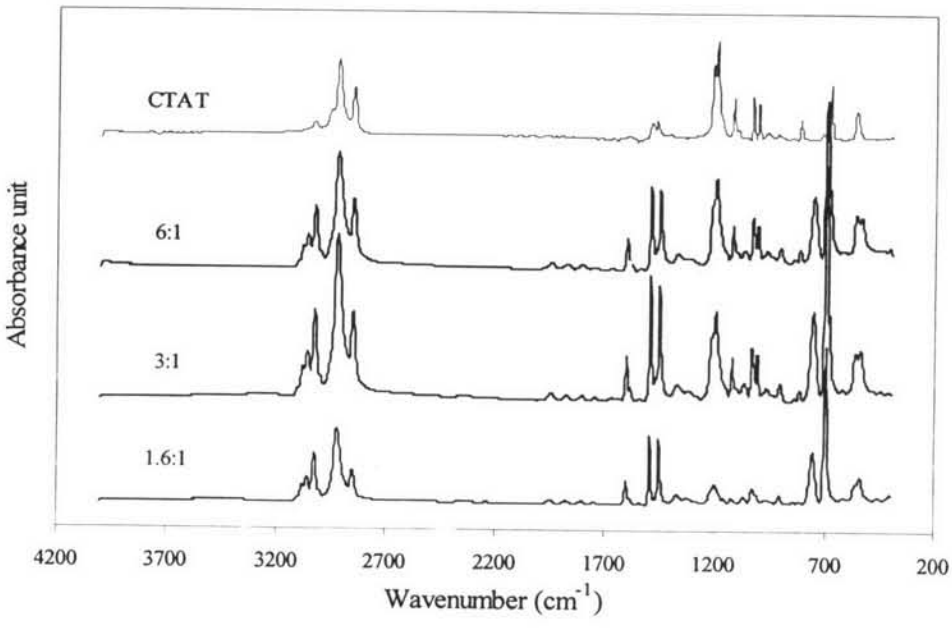

Figure 4.5 FTIR spectrum of CTAT and polystyrene in 20 %wt CTAT and 15:1 of styrene to AIBN.

4.3.2 Thermal Gravimetric Analysis Results

All obtained polymer samples were also examined by thermogravimetric analysis in order to further verify the existence of polystyrene and study the thermal stability of the obtained polymers. The TGA results of obtained polystyrene prepared at different conditions showed a two-step decomposition process. As shown in Figure 4.6, the first weight loss was consistent with the CTAT decomposition at 290-330 °C (see Figure 4.7). The second weight loss was probably be due to polystyrene decomposition at 330 to 430 °C. TGA thermograms of all the polystyrene samples confirmed that polystyrene was successfully polymerized and there were some CTAT surfactant trapped in the polystyrene from precipitation process.

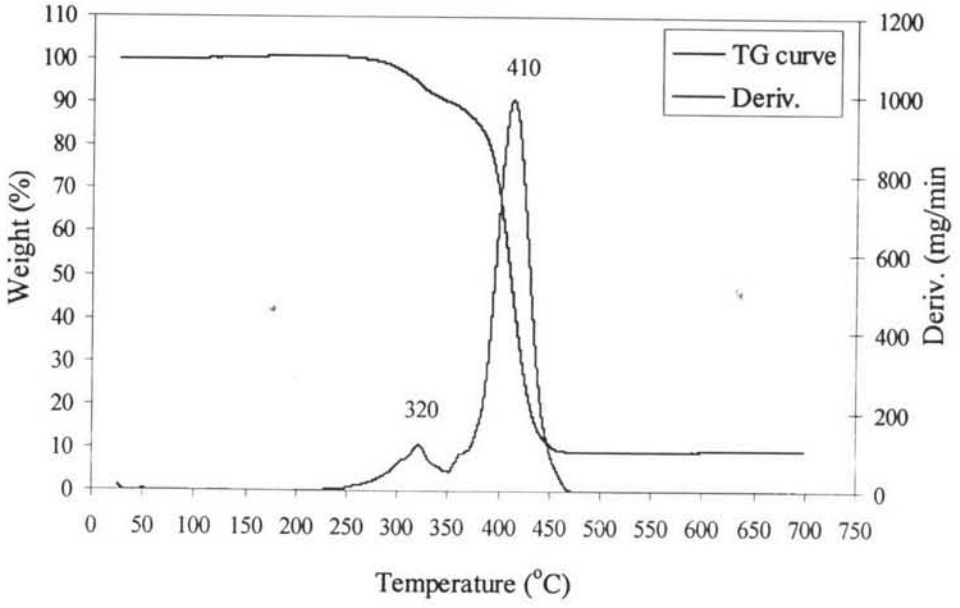

Figure 4.6 TGA thermogram of polystyrene sample in 20 %wt CTAT 1.6:1of CTAT to styrene and 15:1of styrene to AIBN.

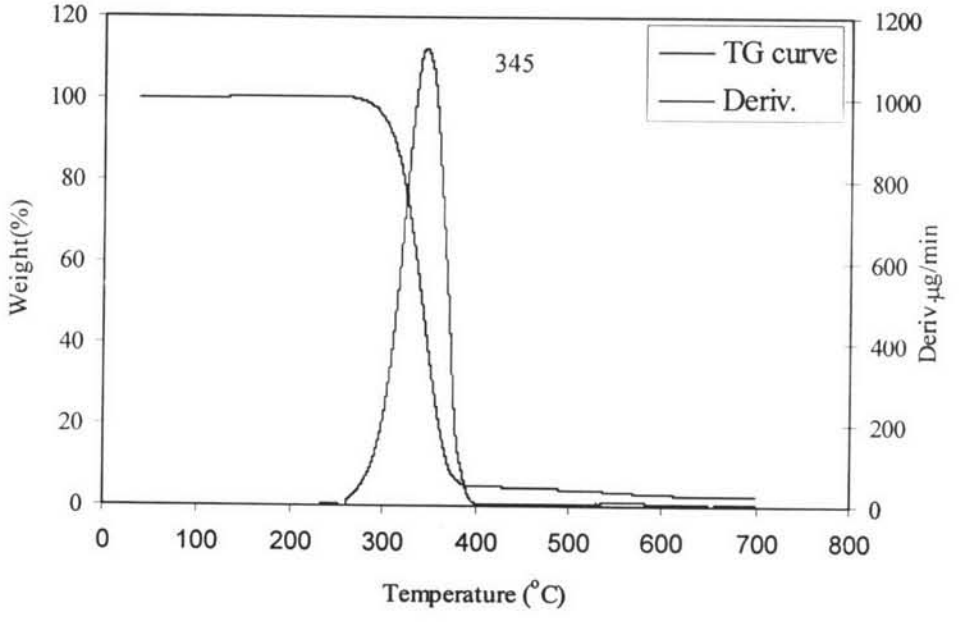

Figure 4.7 TGA thermogram of CTAT

4.3.3 Differential Scanning Calorimeter Results

Differential Scanning Calorimeter was carried out to characterize and study the thermal stability of the obtained polystyrene and CTAT.

Figure 4.8 depicts a DSC thermogram of CTAT. Thermogram from CTAT shows two thermal transitions at 118 °C and 126 °C, suggesting that there were two crystalline structures present in CTAT solid.

The melting enthalpies and peak temperatures of each of polystyrene samples are also illustrated in Figure 4.9, 4.10, and 4.11. It was found that observed polystyrene samples with different CTAT concentrations and different ratios of styrene to AIBN (15:1, 30:1 and 50:1) gave similar melting transitions at 255-259 °C. These transitions were probable due to the melting of CTAT. As expected, the obtained polystyrene were amorphous and no melting transition peak was expected to be observed.

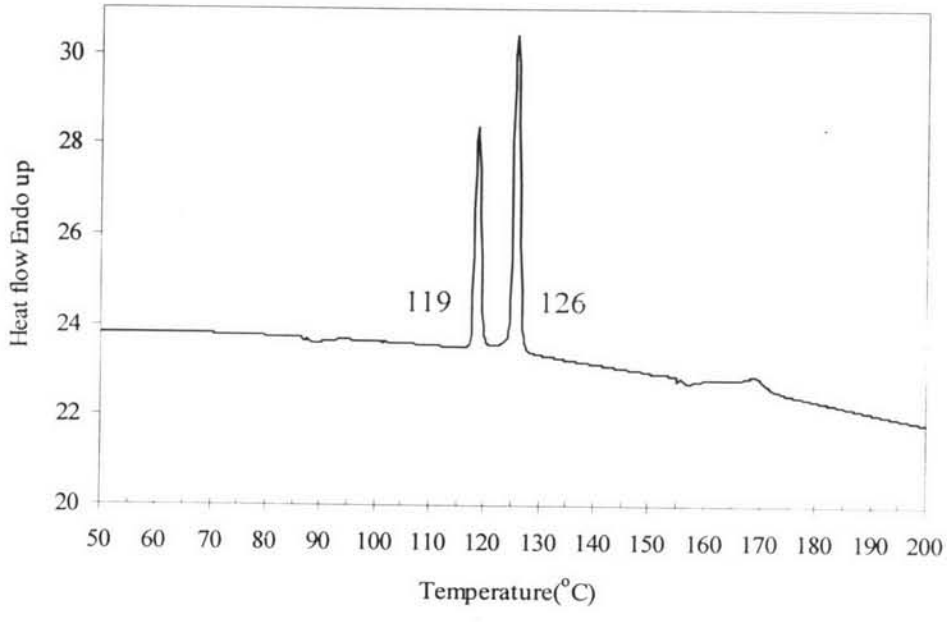

Figure 4.8 The DSC thermogram of CTAT.

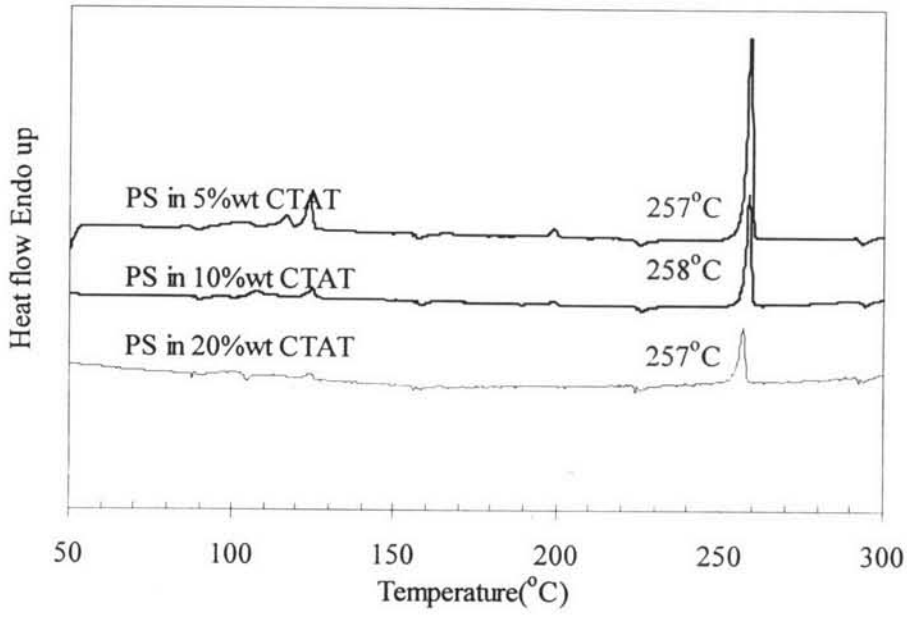

Figure 4.9 The DSC thermogram of polystyrene samples in 15:1 of styrene to AIBN ratios, at high styrene loading.

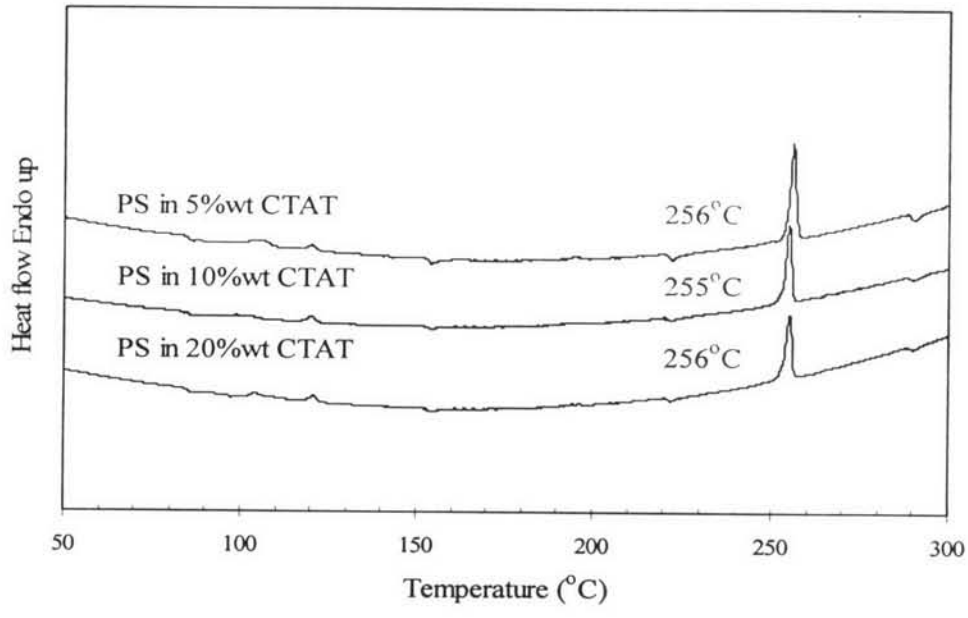

Figure 4.10 The DSC thermogram of polystyrene samples 30:1 of styrene to AIBN ratios, at high styrene loading.

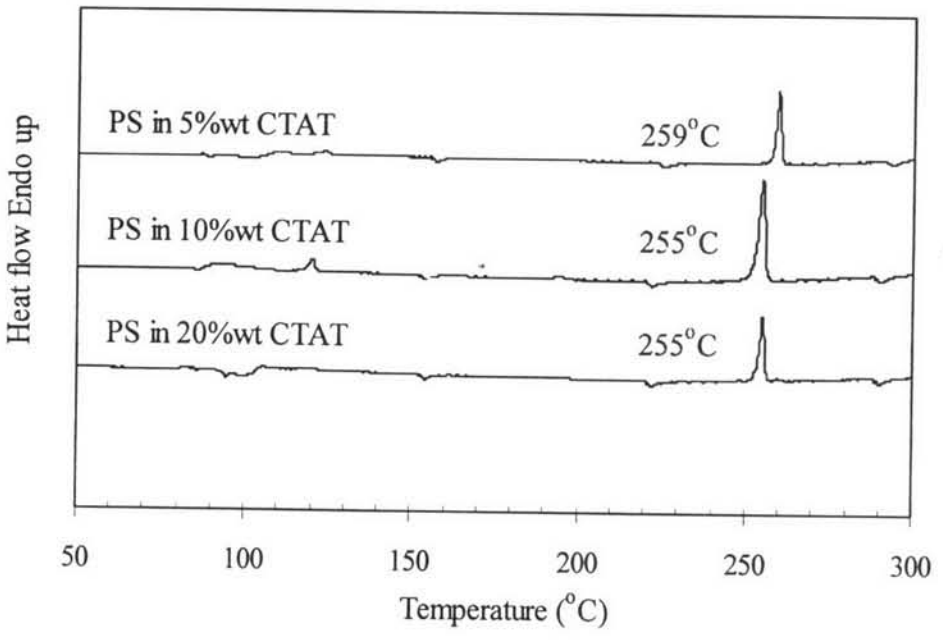

Figure 4.11 The DSC curves of polystyrene samples 50:1 of styrene to AIBN ratios, at high styrene loading.

4.3.4 X-ray Diffraction Results

X-ray diffraction was used to characterize the crystalinity of the obtained polymers and also to further validated results obtained from DSC analysis of the obtained polymers.

Figure 4.12 shows XRD patterns of CTAT sample and polystyrene obtained from 50:1 of styrene:AIBN ratio, at CTAT= 5, 10, and 20 %wt. The XRD results of the obtained polymers clearly show a broad peak consistent with that of amorphous polystyrene and some sharp peaks. These sharp peaks were consistent with the pattern from CTAT sample as shown in Figure 4.12. Results from XRD further confirmed that some CTAT was trapped in the obtained polymers during precipitation process.

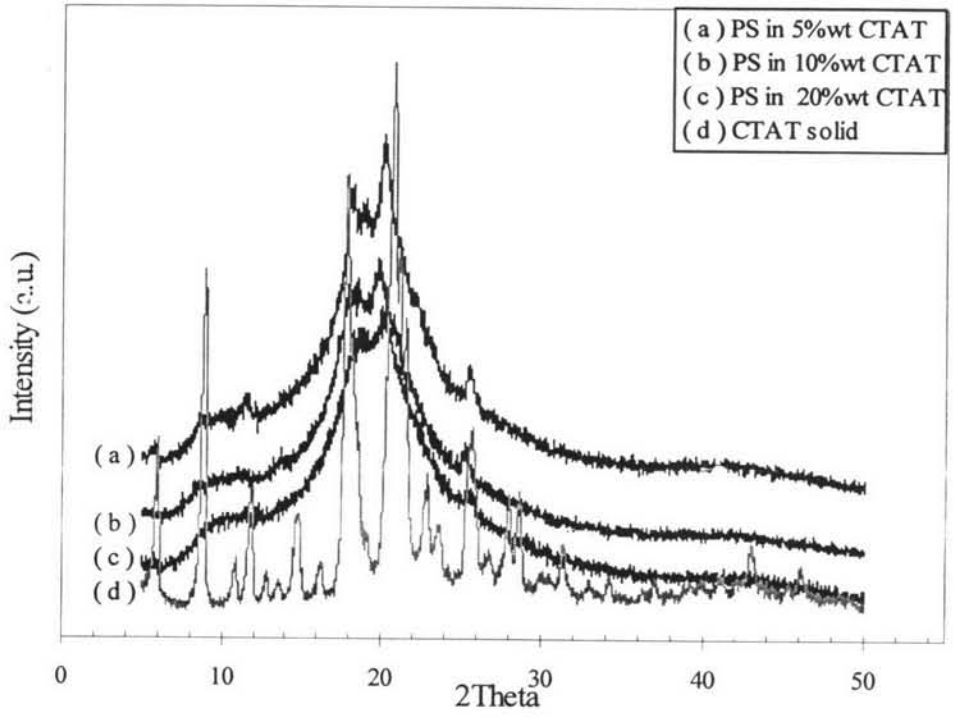

Figure 4.12 WAXD patterns of polystyrene samples (50:1 styrene:AIBN), at high styrene loading and CTAT.

4.3.5 Gel Permeation Chromatography Results

Effect of surfactant concentration, initiator ratio and styrene loading on the molecular weight of polystyrene were determined by GPC using tetrahydrofuran as the solvent. Tables 4.2 and 4.3 show the number average molecular weight ($\overline{M_n}$), weight average molecular weight ($\overline{M_w}$), and molecular weight distribution (MWD) of the obtained polystyrene samples. These samples were obtained from 5 %wt, 10 %wt, and 20 %wt CTAT concentration at different ratios of AIBN loading and styrene loadings.

GPC curves of polystyrene samples showed a single retention time peak indicating a single range of molecular weights was obtained. These peaks were observed in the range of weight average molecular weight ($\overline{M_w}$) between 3,000–700,000 $gmol^{-1}$ and the range of MWD between 3.58-13.87.

Table 4.2 $\overline{M_w}$, $\overline{M_n}$, and MWD of polystyrene samples produced in 5 %wt CTAT

Ratio of CTAT: styrene mol : mol	Ratio of styrene:AIBN mol : mol	Peak		
		$\overline{M_n}$	$\overline{M_w}$	MWD
15:1	6 : 1	N/A	N/A	N/A
	3 : 1	N/A.	N/A	N/A
	1.6 : 1	37533	252024	6.71474
30:1	6 : 1	N/A	N/A	N/A
	3 : 1	N/A	N/A	N/A
	1.6 : 1	63865	394949	6.18606
50:1	6 : 1	N/A	N/A	N/A
	3 : 1	N/A	N/A	N/A
	1.6 : 1	198462	704404	3.549315

N/A= the amount of obtained polystyrene was not enough for characterization.

Table 4.3 $\overline{M_w}$, $\overline{M_n}$, and MWD of polystyrene samples produced in 10 %wt CTAT

Ratio of CTAT: styrene mol : mol	Ratio of styrene:AIBN mol : mol	Peak		
		$\overline{M_n}$	$\overline{M_w}$	MWD
15:1	6 : 1	N/A	N/A	N/A
	3 : 1	13309	100581	7.56142
	1.6 : 1	16731	190215	8.93137
30:1	6 : 1	N/A	N/A	N/A
	3 : 1	N/A	N/A	N/A
	1.6 : 1	689972	194093	5.62838
50:1	6 : 1	N/A	N/A	N/A
	3 : 1	N/A	N/A	N/A
	1.6 : 1	80056	293030	3.66033

N/A= the amount of obtained polystyrene was not enough for characterization.

Table 4.4 $\overline{M_w}$, $\overline{M_n}$, and MWD of polystyrene samples produced in 20 %wt CTAT

Ratio of CTAT: styrene mol : mol	Ratio of styrene:AIBN mol : mol	Peak		
		$\overline{M_n}$	$\overline{M_w}$	MWD
15:1	6 : 1	11429	33355	2.09099
	3 : 1	15681	65376	3.73562
	1.6 : 1	17190	108192	7.24682
30:1	6 : 1	8603	40391	4.73958
	3 : 1	142453	125087	4.07195
	1.6 : 1	16392	22656	13.8678
50:1	6 : 1	198462	704404	3.54932
	3 : 1	12790	120077	9.38415
	1.6 : 1	37084	168239	4.8729

4.3.6 Effect of CTAT Concentration, Monomer Loading, Initiator Loading and Polymerization Temperature

The effects of CTAT concentrations, initiator loadings, and styrene loadings were investigated by GPC to study the impact of these factors on molecular weight of the obtained polystyrene from wormlike micelle and TEM was used to investigate the morphology of the obtained polystyrene stabilized wormlike micelle. The effect of polymerization temperatures, on the changes in micelle structure was also studied by TEM.

4.3.6.1 Effect of CTAT Concentration, Monomer Loading and Initiator Loading on $\overline{M_w}$

Effect of Surfactant Concentration

The preparation of polymer in micelle structures was conducted at the following ratios of CTAT surfactant to styrene monomer (1:6, 1:3,

1:1.6). Figure 4.13 shows the weight average molecular weight of obtained polystyrene as a function of CTAT concentration.

When 5 %wt, 10 %wt and 20 %wt CTAT concentration were studied. At low CTAT concentration (5 %wt), big sphere micelles in the emulsion sample were observed. These could be droplets of monomers in a sphere micelles. At high CTAT concentration (10 %wt and 20 %wt), wormlike micelles were observed. The different morphology of the micelles could have effect on the molecular weight of the polymer as observed in this study. The elongated wormlike micelles made if rather difficult for styrene monomers to collide with one another, thus, the weight average molecular weights of polystyrene in CTAT concentration of 5 %wt. in all AIBN content were higher than 10 %wt's and 20 %wt's.

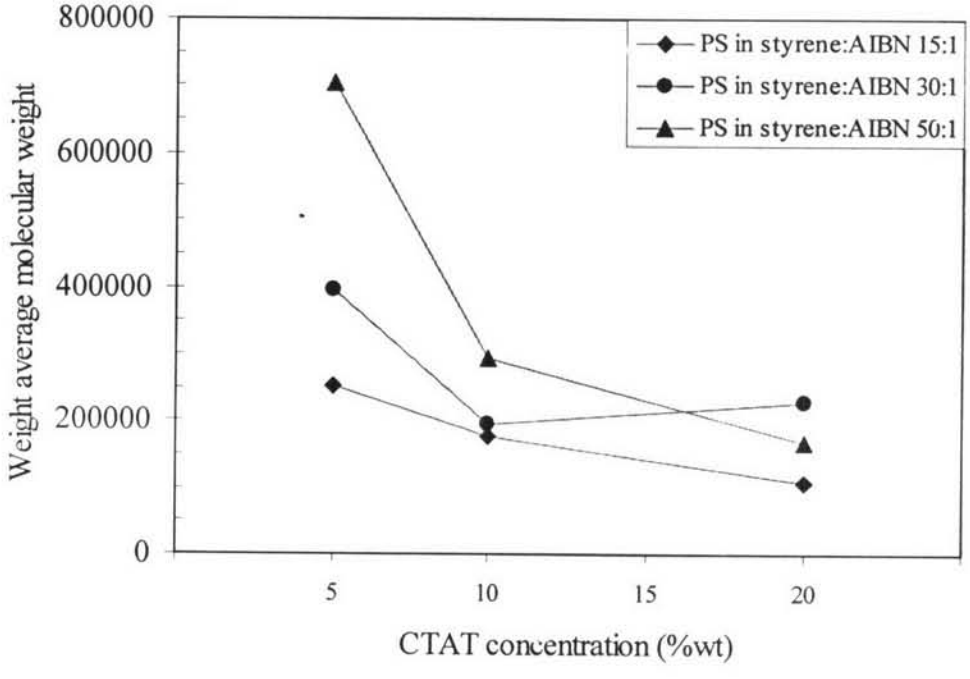

Figure 4.13 Effect of CTAT concentration on weight average molecular weight of polystyrene at high styrene loading (1.6:1).

Effect of Initiator Loading

The preparation of polymer in micelle structures was conducted at the following ratios of styrene monomer to AIBN initiator (15:1, 30:1,

50:1). GPC was used to study effects of initiator loading on the molecular weight of the obtained polystyrene. Figure 4.14 displays the weight average molecular weight of polystyrene in 5 %wt, 10 %wt, and 20 %wt of CTAT concentration with decreasing AIBN loading.

Figure 4.14 shows that as the AIBN loading decreases, the weight average molecular weight of obtained polystyrene tend to increase, as would be expected. More initiator means the formation of more active chains, which would lower the molecular weight of each chain rather quickly. The excess AIBN radicals probably assisted in terminate active polystyrene chains. The results show that at 1:50 of styrene to AIBN ratio produced the highest weight average molecular weight at all CTAT concentrations.

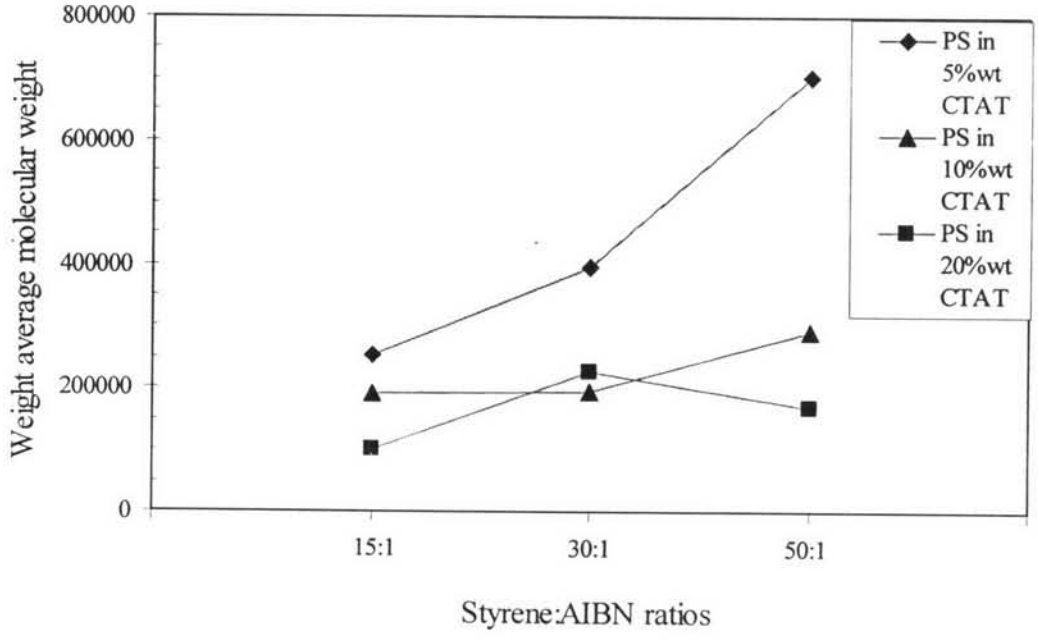

Figure 4.14 Effect of initiator loading on weight average molecular weight of polystyrene in 20 %wt CTAT concentration.

Effect of Styrene Loading

Figure 4.15 shows the effects of styrene loading on weight average molecular weight of polystyrene in CTAT concentration of 20 %wt. The results show that as styrene solubilization within the micelles increased (constant

initiator ratio and temperature), molecular weight of obtained polystyrene also increased. These results were observed in all systems studied. The results could suggest that when solubilized styrene loading increased, the CTAT would be swollen and density of styrene per micelle increased. Thus, the monomers would have greater mobility and were in closer proximity, leading to a relatively high $\overline{M_w}$ polystyrene.

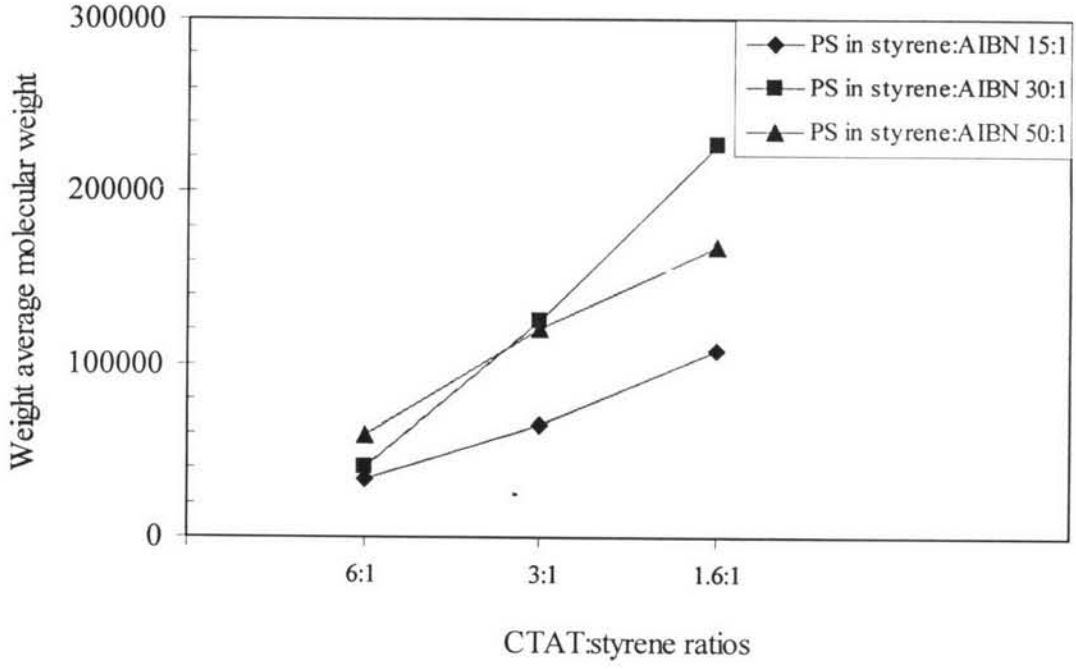

Figure 4.15 Effect of styrene loading on weight average molecular weight of polystyrene.

4.3.6.2 Effect of CTAT Concentration, Monomer Loading, Initiator Loading and Polymerization Temperature on Morphology of Wormlike Micelles

The emulsion polystyrene samples at various conditions were studied by TEM to determine the presence, characteristics and morphology of the stabilized wormlike micelles. The effects of CTAT concentration, AIBN loading, styrene loading, and temperature on the morphology of stabilized wormlike micelles were also investigated using TEM.

Figure 4.16-4.18 show transmission electron photograph of stabilized polystyrene wormlike micelles obtained at 5 %wt, 10 %wt, and 20 %wt CTAT at 15 mole of styrene:1 mole of AIBN, and high styrene loading (1.6:1) and at 70 °C respectively. The results from photographs show that short polystyrene rods were observed in 5 %wt CTAT. The average size was about 3.40 nm in diameter and 32.60 nm in length. In 10 %wt CTAT, the longer rods were observed. The average diameter was 3.73 nm and average length was 57.92 nm The diameter and length of longer rod polystyrene stabilized wormlike micelles in 20 %wt CTAT were 3.75 nm and 59.10 nm respectively.

Figure 4.19-4.21 show transmission electron photographs of stabilized wormlike micelles obtained in 5 %wt, 10 %wt, and 20 %wt CTAT at 30 mole of styrene:1 mole of AIBN, high styrene loading (1.6:1) and 70 °C respectively. The short rods, longer rods, and wormlike micelles were observed for in 5 %wt, 10 %wt, and 20 %wt CTAT respectively. For 5 %wt CTAT, the short polystyrene stabilized micelles rods were 2.91 nm in diameter and 33 nm in length. Typical dimension for longer rod micelles at 10 %wt CTAT were 3.00 nm (diameter) and 41 nm and dimension for wormlike micelles at 20 %wt CTAT were 2.89 nm (diameter) and 47 nm (length).

The polystyrene stabilized micelles samples produced in 5 %wt, 10 %wt, and 20 %wt CTAT at 50 mole of styrene:1 mole of AIBN, high styrene loading (1.6:1), and at 70 °C were shown in Figure 4.22 to 4.24. The obtained results show similar trend to that observed for 15:1 and 30:1 styrene to AIBN ratios. The 5 %wt CTAT long rod polystyrene stabilized micelles were length 4.38 nm in diameter and 47 nm in length. The longer rod polystyrene stabilized micelles observed at 10 %wt CTAT were 2.67 nm in diameter and 60 nm in length. For the longest polystyrene stabilized micelles were obtained from 20 %wt CTAT condition (89 nm in length and 4.6 nm in diameter).

The effects of CTAT surfactant concentration on morphology of polystyrene stabilized wormlike micelles were investigated. Looking at Figure 4.16 to Figure 4.24, at varying CTAT concentrations, the results show that the length of polystyrene stabilized micelles increase with increasing CTAT concentration. At low CTAT concentration, surfactant molecules were assembled to

form spherical micelles while in higher concentrations the micelles grew and the longer micelles were formed, such as rod and wormlike micelles.

Results from Figures 4.16 to Figure 4.24 also demonstrated indicate the effects of AIBN loading. They show that the length of polystyrene stabilized wormlike micelles at a fix CTAT concentration and styrene loading also increase with decreasing AIBN loading. For free-radical polymerization; if the initiator molecules are in excess, they most likely terminate the active polymer chains. More molecules of AIBN produced shorter polystyrene chains, as expected.

In addition the effects of styrene loading were also observed when looking at Figure 4.24, Figure 4.25, and Figure 4.26. Higher styrene loading produced higher molecular weight polymer and longer wormlike micelles. The highest amounts of obtained polystyrene and longest wormlike micelles were prepared in 1.6:1 of CTAT to styrene ratio.

The effect of polymerization temperature can be studied by looking at Figure 4.24, Figure 4.27, and Figure 4.28. Comparing polymerization temperature at 70 °C, 60 °C, and 50 °C at a fix CTAT concentration, AIBN loading and styrene loading, the longest length of polystyrene stabilized micelles was prepared at 70 °C suggesting that AIBN molecules dissociate more rapidly at 70 °C than at 60 °C or 50 °C and thus higher molecular weight polymer was produce and longer polystyrene stabilized wormlike micelles were also produced.

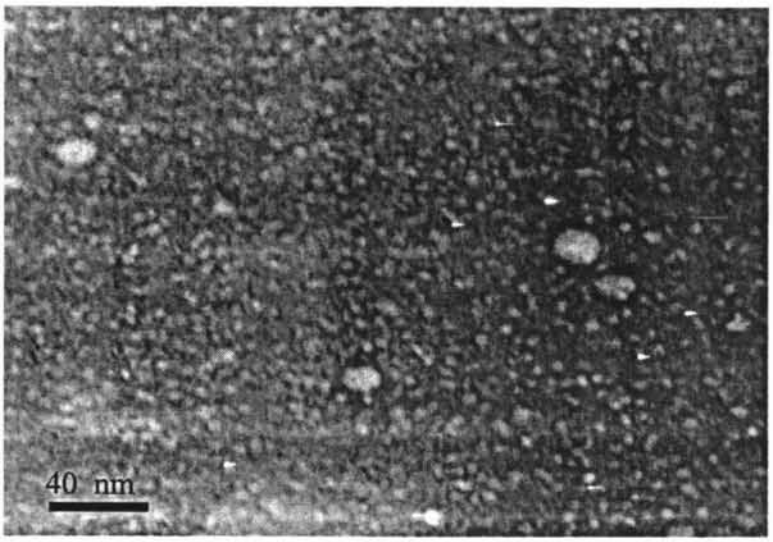

Figure 4.16 Photograph of polystyrene stabilized micelles at 5 %wt CTAT, high styrene loading (1.6:1) and 15 mole of styrene:1mole of AIBN at 70 °C at 60000X magnification.

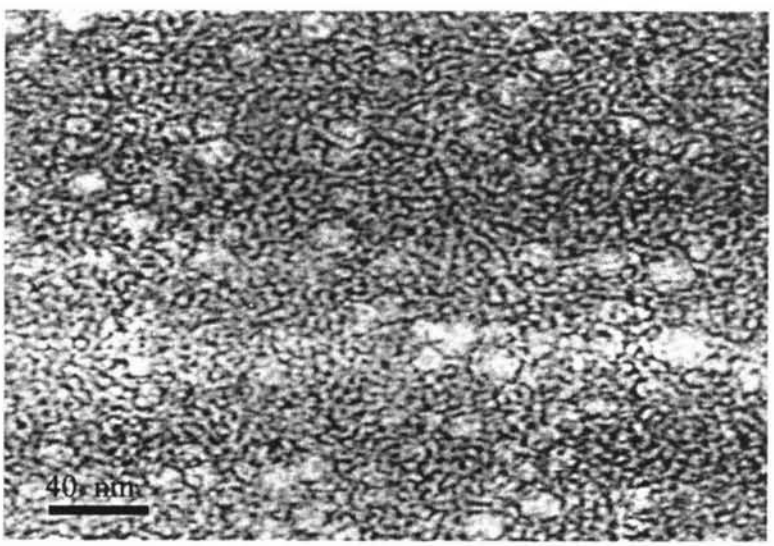

Figure 4.17 Photograph of polystyrene stabilized micelles at 10 %wt CTAT, high styrene loading (1.6:1) and 15 mole of styrene:1mole of AIBN at 70 °C at 60000X magnification.

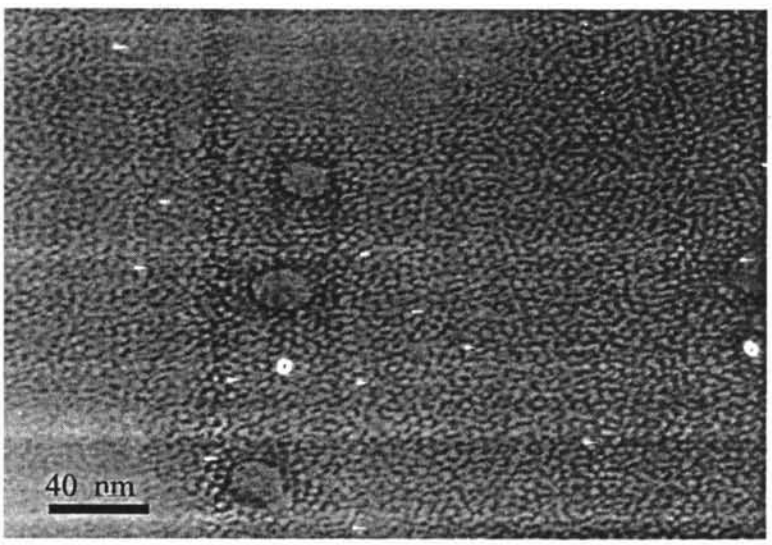

Figure 4.18 Photograph of polystyrene stabilized micelles at 20 %wt CTAT, high styrene loading (1.6:1) and 15 mole of styrene:1mole of AIBN at 70 °C at 60000X magnification.

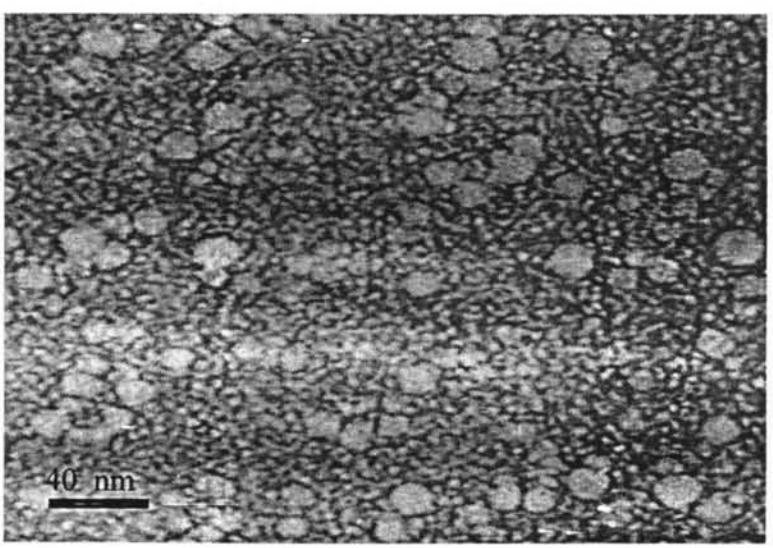

Figure 4.19 Photograph of polystyrene stabilized micelles at 5 %wt CTAT, 30 mole of styrene:1mole of AIBN and high styrene loading (1.6:1) at 70 °C at 60000X magnification.

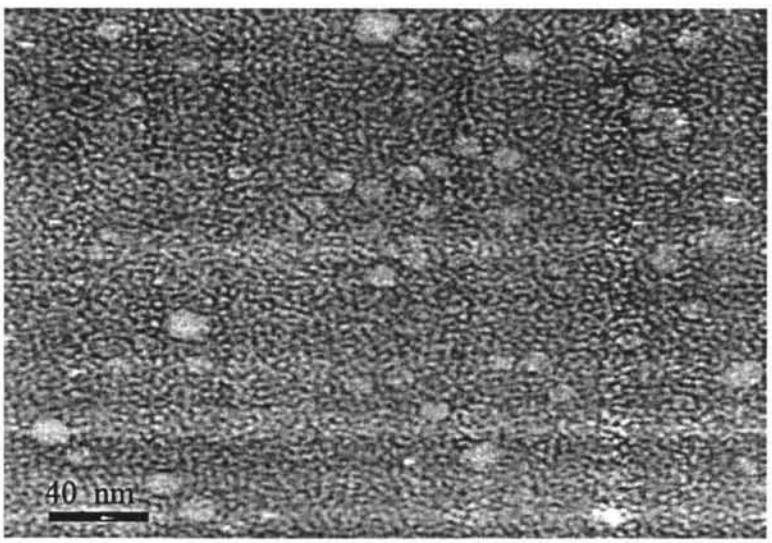

Figure 4.20 Photograph of polystyrene stabilized micelles at 10 %wt CTAT, 30 mole of styrene:1 mole of AIBN and high styrene loading (1.6:1) at 70 °C at 60000X magnification.

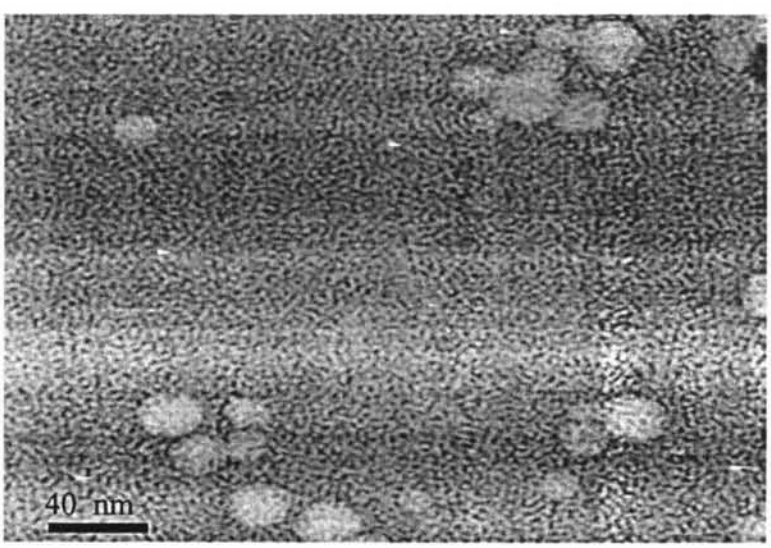

Figure 4.21 Photograph of polystyrene stabilized micelles at 20 %wt CTAT, 30 mole of styrene:1 mole of AIBN and high styrene loading (1.6:1) at 70 °C at 60000X magnification.

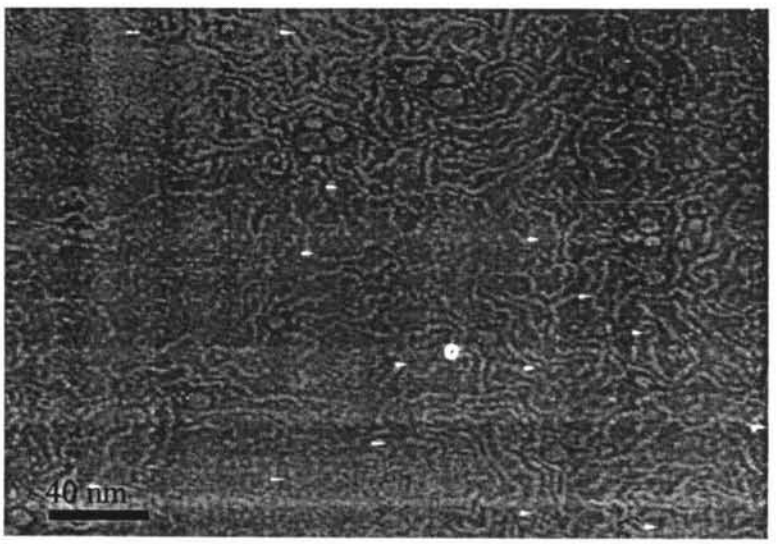

Figure 4.22 Photograph of polystyrene stabilized micelles at 5 %wt CTAT, 50 mole of styrene:1 mole of AIBN and high styrene loading (1.6:1) at 70 °C at 60000X magnification.

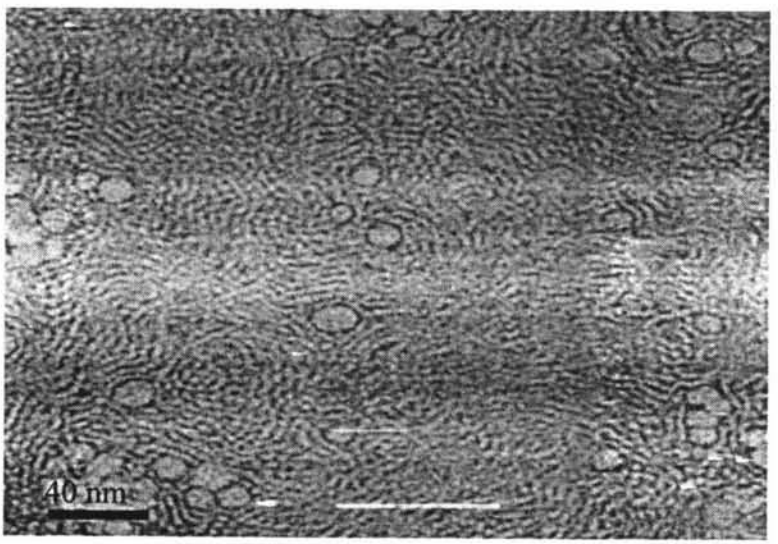

Figure 4.23 Photograph of polystyrene stabilized micelles at 10 %wt CTAT, 50 mole of styrene:1 mole of AIBN and high styrene loading (1.6:1) at 70 °C at 60000X magnification.

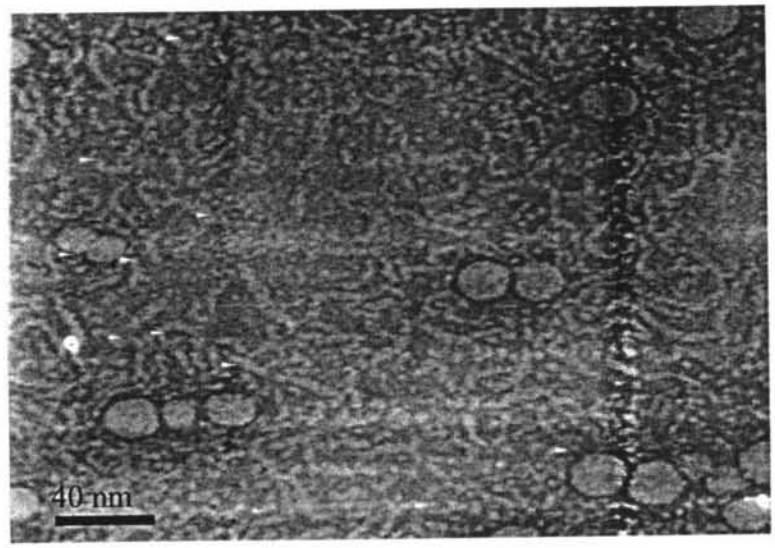

Figure 4.24 Photograph of polystyrene stabilized micelles at in 20 %wt CTAT, 50 mole of styrene:1 mole of AIBN and high styrene loading (1.6:1) at 70 °C at 60000X magnification.

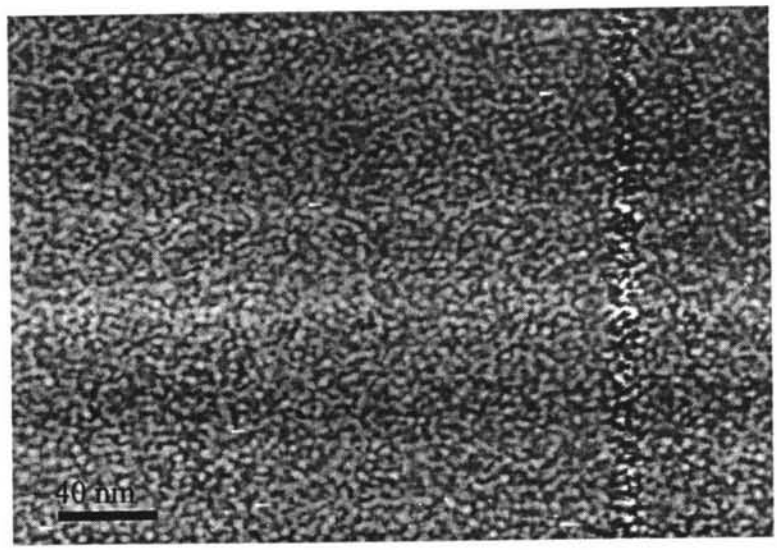

Figure 4.25 Photograph of polystyrene stabilized micelles at in 20 %wt CTAT, 50 mole of styrene:1 mole of AIBN and medium styrene loading (3:1) at 70 °C at 60000X magnification.

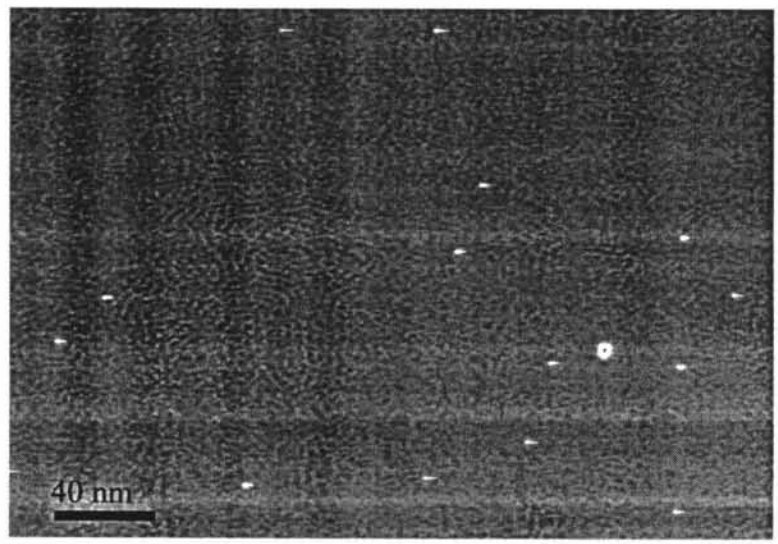

Figure 4.26 Photograph of polystyrene stabilized micelles at 20 %wt CTAT, 50 mole of styrene:1 mole of AIBN and low styrene loading (6:1) at 70 °C at 60000X magnification.

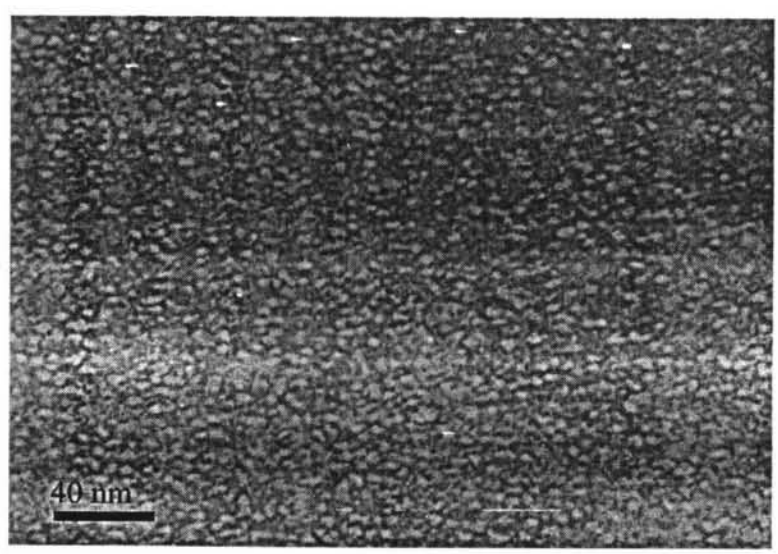

Figure 4.27 Photograph of polystyrene stabilized micelles at 20 %wt CTAT, 50 mole of styrene:1 mole of AIBN and high styrene loading (1.6:1) at 60 °C at 60000X magnification.

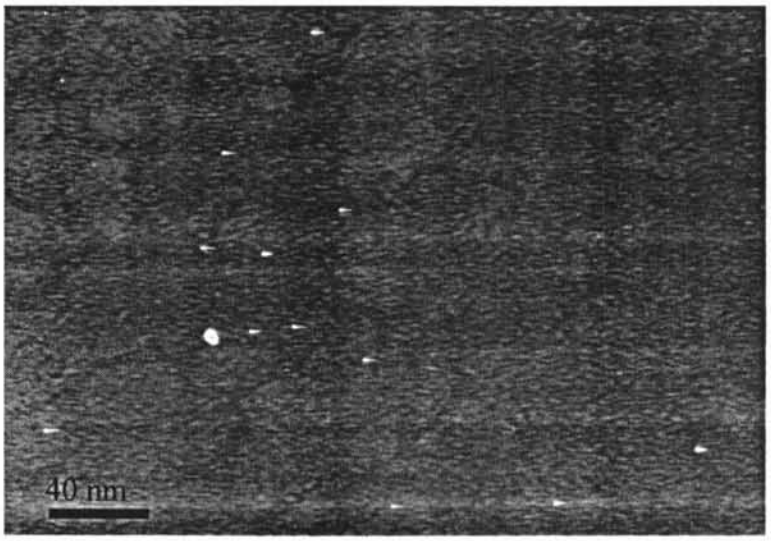

Figure 4.28 Photograph of polystyrene stabilized micelles at 20 %wt CTAT, 50 mole of styrene:1 mole of AIBN and high styrene loading (1.6:1) at 50°C at 60000X magnification.